

Mesoporous Carbon-Supported Pd Nanoparticles in the Metallic State-Catalyzed Acylation of Amides with Aryl Esters via C–O Activation

Hui-Fang Huo, Dan Liu, Agula Bao, Tegshi Muschin, Chaolumen Bai, and Yong-Sheng Bao*



Cite This: *ACS Omega* 2022, 7, 12779–12786



Read Online

ACCESS |



Metrics & More



Article Recommendations



Supporting Information

ABSTRACT: Carbon, an abundant, inexpensive, and nonmetallic material, is an inimitable support in heterogeneous catalysis, and variable carbonaceous materials have been utilized to support metal nanoparticle catalysts. We developed an efficient and stable heterogeneous catalyst with highly dispersed metallic palladium nanoparticles embedded in an ordered pore channel of mesoporous carbon and first applied the catalyst to construct imides from amides using aryl esters as an acylation reagent via C–O activation. The catalyst represents excellent catalytic performance and could be reused and recycled five times without any significant decrease in activity. The heterogeneous nature of metallic state palladium was proven to be the active center in the acylation reaction.



INTRODUCTION

Imides are widely prevalent structural elements present in a variety of organic molecules that exhibit pharmaceutical and bioactive properties.^{1,2} As a consequence, methods for installing imides structure into organic molecules are of great interest, and numerous strategies have been developed to construct those skeletons. In addition, the acylation of the amide with a range of activated acyl species derived from carboxylic acids (such as acid anhydrides and acyl halide) became a widely used method for the synthesis of the imide derivatives, while stoichiometric amounts of salts were produced and the strong base was necessary for those reactions, resulting in the poor atom economy and environmental problems (Scheme 1a).^{3–5} The development of homogeneous catalytic protocols carried the promise of the atom-economical and sustainable formation of imide derivatives, such as the rearrangement of isocyanates, the oxidation of amides, and the oxidative decarboxylation of amino acids. Zhang et al. prepared imides from the oxidation of amides using CuBr as a catalyst and TBHP or TEMPO as an oxidant (Scheme 1b).⁶ Moreover, aldehydes, benzyl alcohol, methyl arenes, and potassium acyltrifluoroborates could also be employed as acylation reagents reacting with amide to afford the desired imides (Scheme 1c).^{7–12} Notably, palladium-catalyzed amino-carbonylation of (hetero) aryl iodides with amides and CO has developed into an alternative reliable protocol for assembling various structurally diverse imides (Scheme 1d).¹³ Although great progress has been realized in this realm, to the best of our knowledge, esters that are readily available and environ-

mentally benign feedstock acting as acylation reagents to synthesize imide derivatives are a formidable challenge.

Environmentally benign, operationally simple, and robust reactions, particularly those employing heterogeneous catalysts, are of significant interest to the chemical industry.^{14–17} Inspired by our previous works which confirmed that supported palladium nanoparticles (PdNPs) could act as heterogeneous catalysts for the amidation reaction between aryl esters with formamides or amines,^{18,19} we hypothesized whether they could serve as a catalyst to construct imide structures using an ester as an acylation reagent.

Carbonaceous materials possess a large specific surface area and good electrical and thermal conductivity and are widely used as supports for heterogeneous catalysts.^{20–26} Metal supported on activated carbons (AC) is one of the most significantly considerable carbon-based catalysts which was studied and applied in chemical engineering.^{27–29} Unfortunately, the mass-transfer process was limited by the microporous structure of activated carbons. The lack of anchor points in the active phase leads to the uneven distribution of the metal nanoparticles on the surface of carbon, easy agglomeration, and leaching. As a result, the synthesis of the

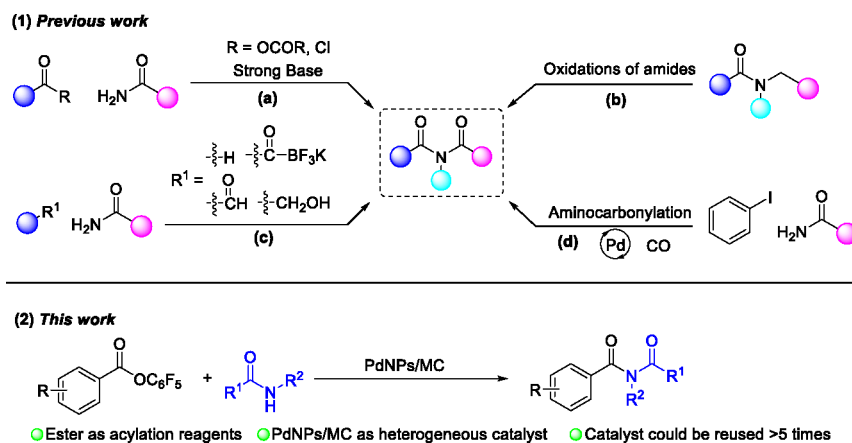
Received: December 28, 2021

Accepted: March 24, 2022

Published: April 7, 2022



Scheme 1. Preparation of Imide Derivates



carbon-supported metal catalyst with adjustable porosity and a high surface area was highly desired.³⁰

Mesoporous carbon (MC) materials could improve the shortcomings of AC, such as insufficient anchor points and the aggregation and leaching of metal nanoparticles through the flexibly adjusted pore size. Also, the strong metal–support interactions triggered by the close contact of metal nanoparticles with the mesoporous material could improve the catalytic activity and stability.^{31–35} Because of the unique physiochemical properties of MC, the mesoporous carbon-supported palladium nanoparticle (PdNP/MC) catalyst has been studied with respect to traditional C–C coupling and hydrogenation reactions. Regrettably, the wide application of the catalyst was hindered by the limited reaction types, poor catalytic performance, and lack of effective preparation methods for completely metallic state PdNPs, which are proven to be active species.^{33,34}

Herein, we prepared various PdNPs/MC catalysts in the metallic state via the impregnation reduction method and first applied these heterogeneous catalysts to facilitate the construction of imide structures using esters as acylation agents via C–O activation, which present a blueprint for the further application of PdNPs/MC in organic synthesis. Compared to commercially available heterogeneous Pd/AC, PdNPs/MC possesses a larger specific surface and exhibits better catalytic performance and stability. The XPS analysis of fresh and used catalyst indicates that the reaction may be performed by a Pd⁰/Pd^{II} catalytic cycle.

RESULTS AND DISCUSSION

Pd nanoparticles immobilized on mesoporous carbon (3 wt % PdNPs/MC) was analyzed by X-ray diffraction (XRD). Clear reflections of fresh and used catalysts (after the fifth recycle) can be observed at 40.0, 46.2, and 68.0° and 39.9, 46.4, and 67.9°, respectively, which correspond well with the (111), (200), and (220) lattice planes of metallic palladium. The diffraction peak intensities of used PdNPs/MC decreased, which may indicate that the particle size of used PdNPs became smaller than that of the fresh catalyst (Figure 1). In addition, the fresh and used catalysts were characterized by the transmission electron microscope (TEM), which showed that the PdNPs were distributed uniformly on the pore channels of MC (Figure 2a,b). The Pd particle size was measured and found to be 5.18 and 4.60 nm for fresh and used catalysts, respectively (Figure 2c,d). A slightly smaller Pd particle size of

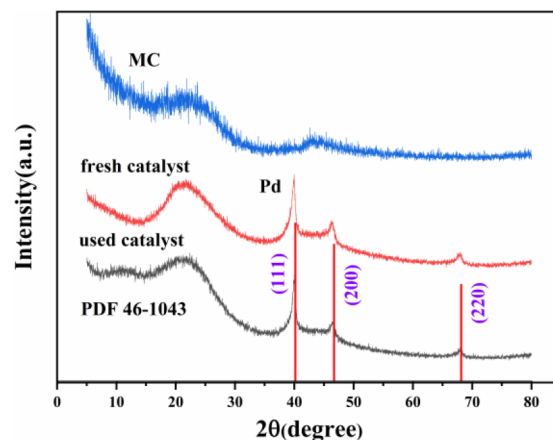


Figure 1. XRD analysis of fresh and used 3 wt % PdNPs/MC.

the used catalyst was observed, in line with the results of XRD analysis.

The PdNPs on the support of fresh and used catalysts exist in the metallic state, which were confirmed by the X-ray photoelectron spectroscopy (XPS) signal that appeared at binding energies of 335.62 eV for Pd 3d_{5/2} and 340.73 eV for Pd 3d_{3/2} over a fresh catalyst and 335.68 eV for Pd 3d_{5/2} and 340.50 eV for Pd 3d_{3/2} over a used catalyst (Figure 3). The binding energies of Pd⁰ in the literature are 335.20 eV for Pd 3d_{5/2} and 340.50 eV for Pd 3d_{3/2}.³⁶ This result confirmed the hypothesis that the PdNPs/MC-catalyzed C–O activation reaction was performed via a catalytic cycle that began with Pd⁰.

The N₂ gas adsorption/desorption analysis of MC, fresh, and used catalysts all exhibit typical type IV adsorption–desorption isotherms. The H2-type hysteresis loops with typical columnar channels at relative pressures of 0.5–0.9 confirmed that fresh and used catalysts both have mesoporous structural features (Figure 4a). The fresh and used catalysts have uniform, small, and arranged mesopores of about 4 nm (Figure 4). The Brunauer–Emmett–Teller (BET) analysis is shown in Table 1. Compared to fresh 3 wt % PdNPs/MC, the smaller specific surface and pore volume of used 3 wt % PdNPs/MC may be attributed to the blockage of the pores by input reaction substrates, which is supported by a comparison of the IR analysis of fresh and used catalysts (Figure 5).

The catalytic properties of the 3 wt % PdNPs/MC were initially evaluated for the acylation of amides (1a) and esters

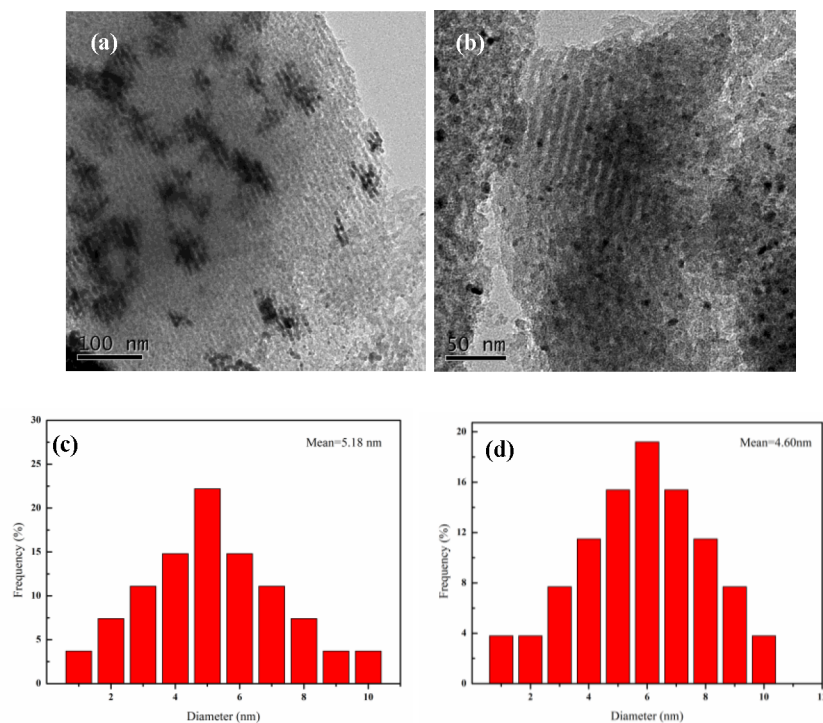


Figure 2. (a) TEM image of fresh 3 wt % PdNPs/MC. (b) TEM image of used 3 wt % PdNPs/MC. (c, d) PdNP size distributions of fresh and used catalysts.

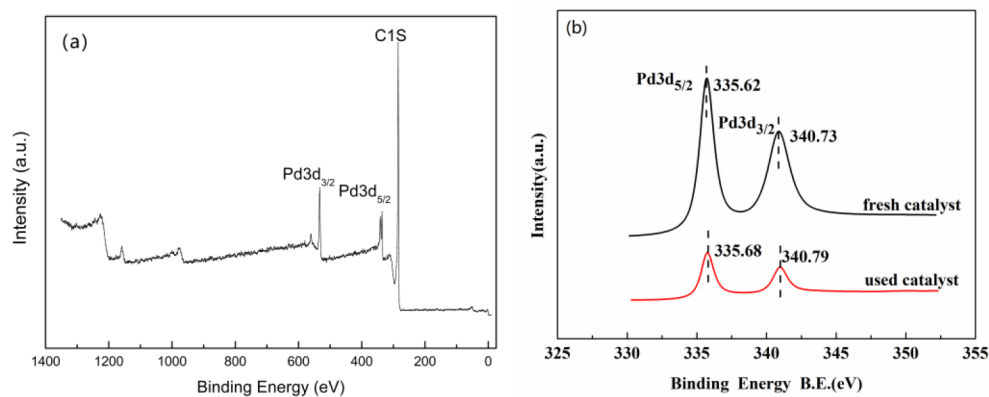


Figure 3. (a) XPS survey of the fresh catalyst. (b) XPS analysis of fresh and used 3 wt % PdNPs/MC.

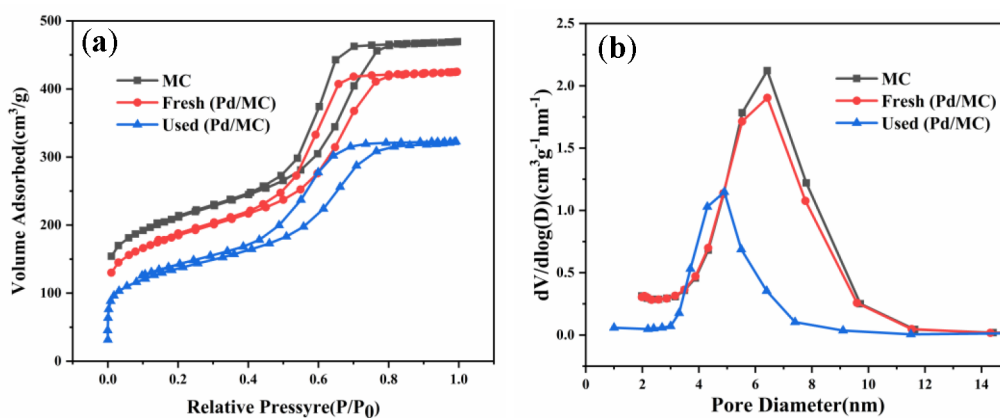
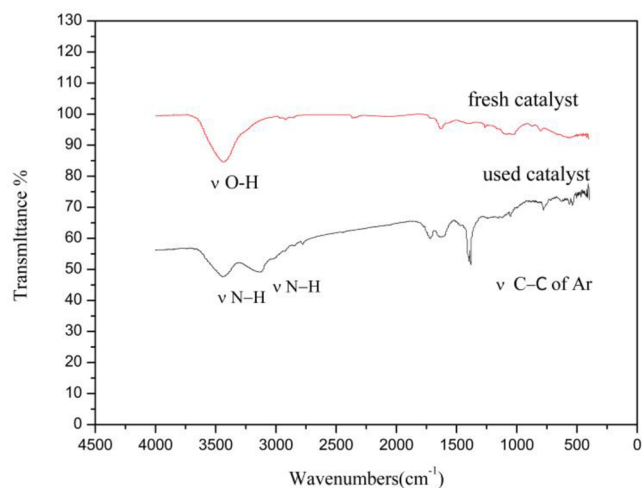


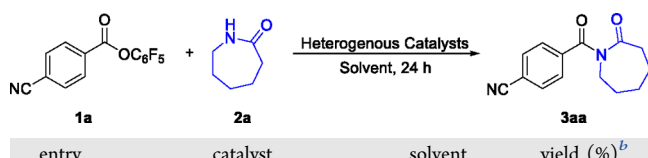
Figure 4. (a) N₂ adsorption/desorption isotherms of MC and fresh 3 wt % PdNPs/MC. (b) Pore size distribution of MC and fresh 3 wt % PdNPs/MC.

Table 1. N₂ Gas Adsorption/Desorption Analysis of Catalysts

sample	specific surface (m ² /g)	pore volume (m ² /g)	pore size (nm)
MC	736	0.72	3.9
fresh (3 wt % PdNPs/MC)	647	0.66	4.0
used (3 wt % PdNPs/MC)	481	0.50	4.2

**Figure 5.** IR analysis of fresh and used catalysts.

(**2a**) in ethyl acetate at 120 °C (Table 2). Initially, commercially available 5 wt % Pd/C was used as the catalyst for the reaction and gave **3a** in 45% yield (entry 1). Pd/ γ -Al₂O₃, an efficient catalyst in our previous work, was also examined and afforded **3a** in 73% yield. Notably, when 3 wt % PdNPs/MC acted as the catalyst for this reaction, gains in

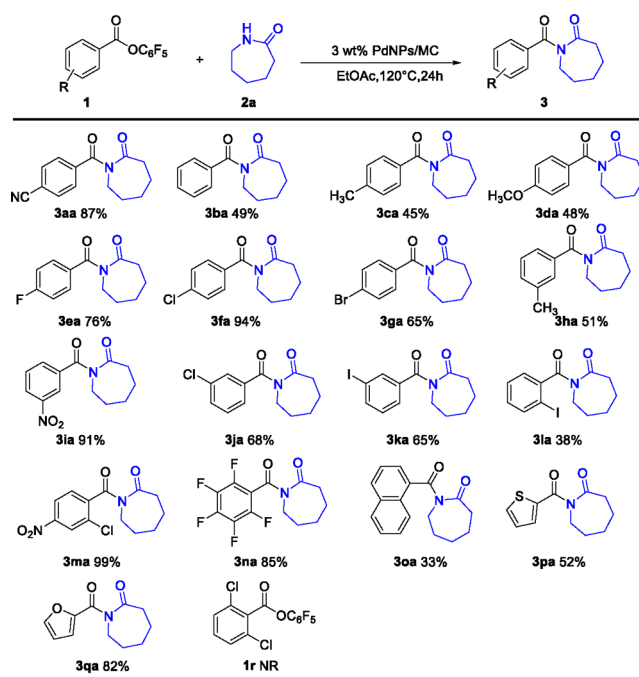
Table 2. Optimization of Reaction Conditions^a

entry	catalyst	solvent	yield (%) ^b
1	5 wt % Pd/AC	EtOAc	45
2	3 wt % Pd/ γ -Al ₂ O ₃	EtOAc	73
3	3 wt % PdNPs/MC	EtOAc	87
4	Pd(OAc) ₂	EtOAc	78
5	3 wt % Pd/PC	EtOAc	35
6	3 wt % Pd/MWCNT	EtOAc	52
7	3 wt % Pd/NMC	EtOAc	52
8	1 wt % PdNPs/MC	EtOAc	31
9	2 wt % PdNPs/MC	EtOAc	48
10	4 wt % PdNPs/MC	EtOAc	65
11	5 wt % PdNPs/MC	EtOAc	48
12	3 wt % PdNPs/MC	PhCl	8
13	3 wt % PdNPs/MC	MeCN	23
14	3 wt % PdNPs/MC	EtOH	35
15	MC	EtOAc	
16 ^c	3 wt % PdNPs/MC	EtOAc	63
17 ^d	3 wt % PdNPs/MC	EtOAc	42

^aReaction conditions: **1a** (0.1 mmol), **2a** (3 equiv), catalyst (25 mg), EtOAc (0.5 mL), 24 h, 120 °C. ^bIsolated yields. ^c130 °C. ^d100 °C.

yields were observed, which could afford the desired products in 87% yield (entry 3), presumably owing to the comprehensive larger specific surface area of 3 wt % PdNPs/MC. Employing Pd(OAc)₂ led to a slight decrease in the yield of the reaction (entry 4). PdNPs supported on different carbon materials, such as porous carbon, multiwalled carbon nanotubes (MWCNT), N-doped mesoporous carbon materials (NMC), and porous carbon (PC), can also be applied to the reaction, albeit in lower yields (entries 5–7). Any fluctuation in the Pd content of MC from 3 wt % (1, 2, 4, and 5 wt %) resulted in a decrease in reaction yields (entries 8–11). A brief screening of solvents suggested that EtOAc is the optimal solvent (entries 12–14). Omitting Pd failed to afford even trace amounts of the desired product (entries 15). Changing the reaction temperature offered poor yields (entries 16 and 17).

With optimal reaction conditions in hand, we explore the versatility of aryl esters. As illustrated in Table 3, a series of

Table 3. Versatility of Aryl Esters^{a,b}

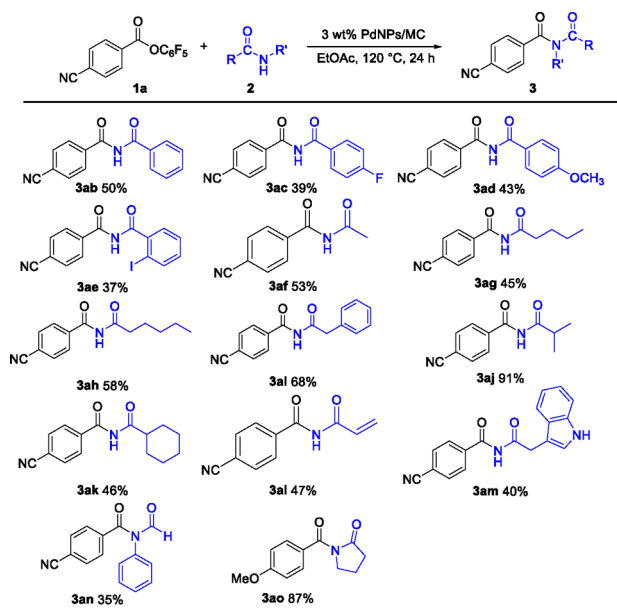
^aReaction conditions: **1b** (0.1 mmol), **2** (3 equiv), 3 wt % PdNPs/MC (25 mg), EtOAc (0.5 mL), 24 h, 120 °C. ^bIsolated yields.

substituted aryl esters allow the reaction to proceed smoothly to afford the desired products in moderate to excellent yields. An aryl ester bearing an electron-withdrawing group or an electron-donating group at the *para* or *meta* position as well as multiple substituents gave the desired products in moderate to excellent yields (**3aa–3na**). Interestingly, a preference for the electron-withdrawing groups on the phenyl group of an aryl ester was observed for this reaction (**3ea–3ga** vs **3ca–3da**). The strong electron-deficient aryl esters exhibited excellent reactivity and afforded the desired imides at up to 99% yield (**3ia**, **3ma**, and **3na**). However, substrates with *ortho*-substituted groups delivered the products in relatively lower yields, which might be attributed to the steric hindrance (**3la**) and thus substrate **1r** with two *-Cl* substituents in the *ortho* position of the ester group failed to give any expected products. Fortunately, substrates containing a heteroaryl ring were

suitable for this protocol, providing products in moderate yields (**3pa** and **3qa**).

Subsequently, the scope and limitations of amide **2** were examined using **1a** as the coupling partner (Table 4). An aryl

Table 4. Scope of Amides^{a,b}



^aReaction conditions: **1b** (0.1 mmol), **2** (3 equiv), 3 wt % PdNPs/MC (25 mg), EtOAc (0.5 mL), 24 h, 120 °C. ^bIsolated yields.

amide with electron-donating or electron-withdrawing groups (4-F, 4-OCH₃, and 2-I) participated in the reaction to afford the desired product in moderate yields (**3ab–3ae**). A range of primary amides containing different alkyl groups display relatively better reaction efficiencies, furnishing imides in moderate to excellent yields (**3af–3ak**). Satisfactorily, an amide with terminal alkenes gave an imide in 47% yield, thereby offering an opportunity for further derivatization. In addition, the 1*H*-indene containing an internal alkene was also tolerated in this protocol and converted to the **3am** product, albeit in a somewhat low yield. Notably, *N*-phenylformamide served as a suitable substrate for this reaction (**3an**, 35% yield). Imides are widespread in pharmaceuticals. We could construct aniracetam, a drug improving brain function, in 87% yield (**3ao**).

The ester bearing different aryl groups was tested (Scheme 2). Changing pentafluorophenyl to an ester pyridyl could also afford desired product **3ea**. Furthermore, the electron-deficient aryl picolinates are also compatible in the reaction.

The possibility of the recyclability of the 3 wt % PdNPs/MC in this reaction was also investigated using substrates **1a** and **2a** under optimal reaction conditions. As illustrated in Figure 6, the heterogeneous catalyst could be recovered by centrifugation and reused five times without any dramatic decrease in catalytic efficiency, and a slight decrease in yield was observed for the fifth cycle.

This protocol appeared to operate mainly by heterogeneous pathways, as demonstrated by a hot filtration test. After filtering the 3 wt % PdNPs/MC in the middle of the reaction, no further reaction was observed, precluding the possibility of homogeneous catalysis, which was confirmed by the TOF value of **1a**, as shown in Table 5. This result was also proven by

Scheme 2. Scope of Other Esters

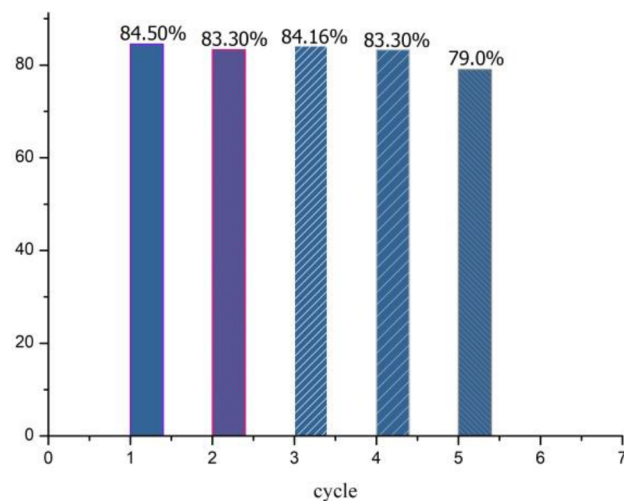
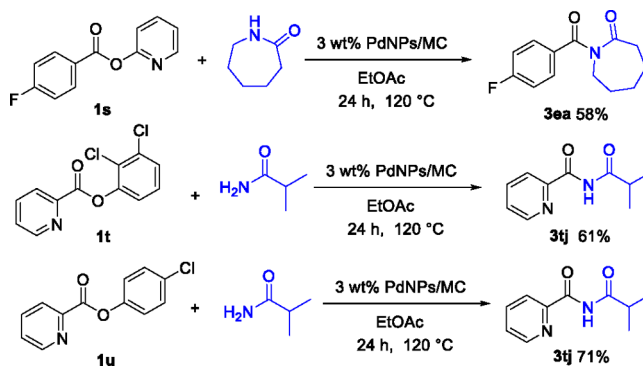


Figure 6. Recyclability of the catalyst.

Table 5. Results of the Hot Filtration Test

time (h)	conversion (%) ^a	TOF
0	0	0
2	35.4	9.61
4 (after hot filtration)	36.1	9.67

^aGC data.

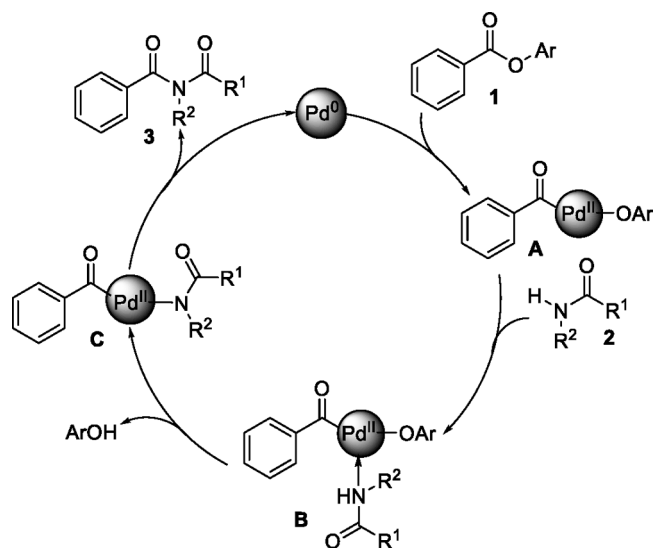
a Hg(0) poisoning test (ESI). The ICP-MS analysis indicated 6.08 ppm Pd leaching into the reaction solution, thus further supporting the stability of the heterogeneous catalyst.

On the basis of previous reports,^{19,37,38} we proposed a plausible mechanism for the acylation of amide (Scheme 3). First, the process would begin with the oxidative addition of Pd⁰ and the C(acyl)–O bond of aryl ester **1**, generating Pd^{II} intermediate A. Subsequently, intermediate A would coordinate with amide to give intermediate B. Then the alkoxide attacked the hydrogen of the amide, resulting in phenol and generating intermediate C. The reductive elimination of intermediate C would generate the imide products and the Pd⁰ catalyst.

CONCLUSIONS

We have prepared an MC-supported metallic state heterogeneous Pd catalyst which would be applied successfully to construct imides from aryl esters and amides via C–O bond activation. This catalyst represents excellent catalytic activity and can be reused and recycled five times without any

Scheme 3. Proposed Reaction Mechanism



significant decrease in activity. The morphology of fresh and used catalysts was investigated by XRD, XPS, TEM, and N_2 gas adsorption/desorption. The XPS analysis of fresh and used catalyst suggested that Pd^0 was the active species. These findings provide an avenue for the wide application of the PdNPs/MC catalysts in undeveloped areas, including C–O, C–N, and C–H activation reactions.

EXPERIMENTAL SECTION

Mesoporous Carbon Preparation. Resorcinol (30 mmol) and F127 (0.4 mmol) were dissolved in a mixed solution of absolute ethanol and ultrapure water (40 mL, $V_{H_2O}/V_{EtOH} = 1:1$), and then concentrated HCl (mass fraction 37%, 4 mmol) was added to the mixture, which was stirred at room temperature for 1 h. Formaldehyde solution (mass fraction 37%, 60 mmol) was added dropwise to the solution and stirred vigorously for another hour at room temperature. The resulting mixed solution was transferred to the reactor that was placed in an oven at 100 °C for 3 days. The rough product was cooled to room temperature, washed via centrifugation three times with water, and dried overnight at 80 °C. The obtained solid was carbonized for 3 h at 600 °C under a nitrogen atmosphere in a tube furnace at a heating rate of 2 °C/min. The product was cooled to room temperature and ground to obtain a black powder.³⁹

Porous Carbon Preparation. *p*-Phenylenediamine (0.01 mol) was added to DMF (70 mL) at room temperature under magnetic stirring. After the *p*-phenylenediamine completely dissolved, 3,3',4,4'-benzophenone tetracarboxylic dianhydride (BTDA) (0.01 mol) and ethylenediamine (0.01 mol) were added to the mixed solution in succession and stirred at room temperature for 12 h. The mixture was transferred to an autoclave to react at 150 °C for 12 h, cooled to room temperature, centrifuged at 3900 rpm for 15 min, washed sequentially with ethanol and DMF, and then dried at 60 °C in vacuum for 24 h. Finally, the solid was cooled to room temperature and calcined in a quartz tube furnace at 350 °C for 1 h under a N_2 atmosphere at a 2 °C/min heating rate to complete the activation. The solid was then pyrolyzed at 900 °C for 2 h under a N_2 atmosphere at a heating rate of 2 °C/min to form a porous carbon material.⁴⁰

Doped Mesoporous Carbon Preparation. Hexamethylenetetramine (4.2 g) was added to a solution of resorcinol (30 mmol) and F127 (0.4 mmol) in a mixed solution of dry ethanol and ultrapure water ($V_{ultrapure\ water}/V_{dry\ ethanol} = 1:1$, 40 mL), and then concentrated hydrochloric acid (37 wt %, 4 mmol) was added to the mixture and stirred at room temperature for 1 h. Formaldehyde solution (37 wt %, 60 mmol) was added dropwise to the solution and stirred vigorously for 1 h under the same conditions. The resulting mixture was transferred to the reaction kettle, reacted in an oven at 100 °C for 3 days, cooled to room temperature, and centrifuged, and the solid was washed with water three times and dried overnight at 80 °C. The obtained solid was carbonized for 3 h in a tube furnace at 600 °C under nitrogen (heating rate of 2 °C/min), cooled to room temperature, and ground to obtain a black powder.³⁹

Heterogenous Catalyst Preparation. The Pd NPs on MC and other supports such as γ - Al_2O_3 and multiwalled carbon nanotubes (MWCNTs) were prepared by the modified impregnation–reduction method. A PdNPs/MC heterogeneous catalyst (3 wt %) was prepared by the following procedure: a solid support (0.97 g) was suspended in distilled water (50 mL), followed by adding $PdCl_2$ aqueous solution (0.01 M, 28.2 mL) and stirring at room temperature. Then an L-lysine aqueous solution (0.03 M, 1 mL) was added to this mixture. Subsequently, a NaOH aqueous solution (0.1 M) was added to the mixture to adjust the pH to 7 before being treated with a $NaBH_4$ aqueous solution (0.35 M, 4.5 mL) dropwise within 10 min with vigorous stirring. The mixture was aged for 24 h and centrifuged to afford a solid, which was washed four times with distilled water and once with ethanol before being dried at 80 °C. The dried solid was used directly as the catalyst.

Activity Test. The acylation of 4-cyanobenzoic acid pentafluorophenol ester **1a** with caprolactam **2a** was used as a model reaction. In a typical reaction, 3 wt % PdNPs/MC (25 mg), **1a** (31.3 mg, 0.10 mmol), **2a** (33.9 mg, 0.3 mmol), and EtOAc (0.5 mL) were added to a 25 mL oven-dried reaction tube. The resulting solution was stirred at 120 °C for 24 h via a magnetic stirrer. The crude product was concentrated under reduced pressure and purified by column chromatography to afford desired product **3**.

Catalyst Recycling Experiment. After each reaction cycle, the solvent, substrate, and products were removed by centrifugation; the separated 3 wt % PdNPs/MC was washed thoroughly with 0.1 M NaOH ethanol solution (twice) and distilled water (four times) and then washed twice with ethanol, followed by centrifugal separation and drying at 80 °C for 12 h. The recovered catalyst was used for the next cycle.

Hot Filtration Test. PdNPs/MC (25 mg, 3 wt %), 4-cyanobenzoic acid pentafluorophenol ester (31.3 mg, 0.10 mmol), caprolactam (33.9 mg, 0.3 mmol), and EtOAc (0.5 mL) were added to the reaction tube. The resulting solution was stirred at 120 °C for 2 h in a magnetic stirrer, and the reaction mixture was filtered through a preheated Celite pad after the reaction for 2 h. The filtrate was detected by GC to obtain the conversion of **1a** and TOF. Then the filtered reaction solution continued to react for 2 h under normal conditions and was detected by GC again.

ASSOCIATED CONTENT

Supporting Information

The Supporting Information is available free of charge at <https://pubs.acs.org/doi/10.1021/acsomega.1c07342>.

General experimental information; methods of analysis and a list of reagents; characterization of all compounds; and ^1H and ^{13}C NMR spectra for each compound (PDF)

AUTHOR INFORMATION

Corresponding Author

Yong-Sheng Bao – College of Chemistry and Environmental Science, Inner Mongolia Key Laboratory of Green Catalysis, Inner Mongolia Normal University, Hohhot 010022, China; orcid.org/0000-0002-6686-7171; Email: sbbys197812@163.com

Authors

Hui-Fang Huo – College of Chemistry and Environmental Science, Inner Mongolia Key Laboratory of Green Catalysis, Inner Mongolia Normal University, Hohhot 010022, China

Dan Liu – College of Chemistry and Environmental Science, Inner Mongolia Key Laboratory of Green Catalysis, Inner Mongolia Normal University, Hohhot 010022, China

Agula Bao – College of Chemistry and Environmental Science, Inner Mongolia Key Laboratory of Green Catalysis, Inner Mongolia Normal University, Hohhot 010022, China;

orcid.org/0000-0002-7859-9960

Tegshi Muschin – College of Chemistry and Environmental Science, Inner Mongolia Key Laboratory of Green Catalysis, Inner Mongolia Normal University, Hohhot 010022, China;

orcid.org/0000-0002-1571-3738

Chaolumen Bai – College of Chemistry and Environmental Science, Inner Mongolia Key Laboratory of Green Catalysis, Inner Mongolia Normal University, Hohhot 010022, China

Complete contact information is available at:

<https://pubs.acs.org/10.1021/acsomega.1c07342>

Author Contributions

H.F.H. and D.L. contributed equally.

Notes

The authors declare no competing financial interest.

ACKNOWLEDGMENTS

We are grateful for financial support from the National Natural Science Foundation of China (21861030), the Inner Mongolia Nature Science Foundation (2021MS02030 and 2020LH02010), the Special Founded Project for Cultivating Major Project of Inner Mongolia Normal University (2020ZD02), the Innovative and Entrepreneurial Startup Supporting Program of Returned Overseas Scholars of Inner Mongolia Autonomous Region, the Collaborative Innovation Center for Water Environmental Security of Inner Mongolia Autonomous Region (XTCX003), the Science and Technology Program of Inner Mongolia Autonomous Region (2020PT0003), and the High-Level Personnel Fund Project of Inner Mongolia Normal University (2019YJRC011). This article is dedicated to the 70th anniversary of Inner Mongolia Normal University.

REFERENCES

- (1) Nakamura, K.; Kurasawa, M. Anxiolytic effects of aniracetam in three different mouse models of anxiety and the underlying mechanism. *Eur. J. Pharmacol.* **2001**, *420*, 33–43.
- (2) Stec, J.; Huang, Q.; Pieroni, M.; Kaiser, M.; Fomovska, A.; Mui, E.; Witola, W. H.; Bettis, S.; McLeod, R.; Brun, R.; Kozikowski, A. P. Synthesis, Biological Evaluation, and Structure-Activity Relationships of N-Benzoyl-2-hydroxybenzamides as Agents Active against *P. falciparum* (K1 strain), Trypanosomes, and Leishmania. *J. Med. Chem.* **2012**, *55*, 3088–3100.
- (3) Lee, J.; Hong, M.; Jung, Y.; Cho, E. J.; Rhee, H. Synthesis of 1,3,5-trisubstituted-1,2,4-triazoles by microwave-assisted N-acylation of amide derivatives and the consecutive reaction with hydrazine hydrochlorides. *Tetrahedron* **2012**, *68*, 2045–2051.
- (4) Wang, F.; Liu, H.; Fu, H.; Jiang, Y.; Zhao, Y. Highly Efficient Iron(II) Chloride/N-Bromosuccinimide-Mediated Synthesis of Imides and Acylsulfonamides. *Adv. Syn. & Catal.* **2009**, *351*, 246–252.
- (5) Wolfe, J. F.; Trimitsis, G. B. Twofold acylations of certain amides by means of sodium hydride. *J. Org. Chem.* **1968**, *33*, 894–896.
- (6) Yu, H.; Chen, Y.; Zhang, Y. TBHP/TEMPO-Mediated Oxidative Synthesis of Imides from Amides. *Chin. J. Chem.* **2015**, *33*, 531–534.
- (7) Aruri, H.; Singh, U.; Kumar, S.; Kushwaha, M.; Gupta, A. P.; Vishwakarma, R. A.; Singh, P. P. I₂/Aqueous TBHP-Catalyzed Coupling of Amides with Methylarenes/Aldehydes/Alcohols: Metal-Free Synthesis of Imides. *Org. Lett.* **2016**, *18*, 3638–3641.
- (8) Bian, Y. J.; Chen, C. Y.; Huang, Z. Z. Synthesis of imides by palladium-catalyzed C-H functionalization of aldehydes with secondary amides. *Eur. J. Chem.* **2013**, *19*, 1129–1133.
- (9) Kataoka, K.; Wachi, K.; Jin, X.; Suzuki, K.; Sasano, Y.; Iwabuchi, Y.; Hasegawa, J. Y.; Mizuno, N.; Yamaguchi, K. CuCl/TMEDA/nor-AZADO-catalyzed aerobic oxidative acylation of amides with alcohols to produce imides. *Chem. Sci.* **2018**, *9*, 4756–4768.
- (10) Wang, J.; Liu, C.; Yuan, J.; Lei, A. Fe-Catalyzed oxidative C-H/N-H coupling between aldehydes and simple amides. *Chem. Commun.* **2014**, *50*, 4736–4739.
- (11) Galvez, A. O.; Schaack, C. P.; Noda, H.; Bode, J. W. Chemoselective Acylation of Primary Amines and Amides with Potassium Acyltrifluoroborates under Acidic Conditions. *J. Am. Chem. Soc.* **2017**, *139*, 1826–1829.
- (12) Yu, H.; Zhang, Y. Copper-Catalyzed Synthesis of Imides from Aldehydes or Alcohols and Amine Hydrochloride Salts. *Eur. J. Org. Chem.* **2015**, *2015*, 1824–1828.
- (13) Ran, L.; Ren, Z. H.; Wang, Y. Y.; Guan, Z. H. Palladium-catalyzed aminocarbonylation of aryl iodides with amides and N-alkyl anilines. *Chem-Asian J.* **2014**, *9*, 577–583.
- (14) Biffis, A.; Centomo, P.; Del Zotto, A.; Zecca, M. Pd Metal Catalysts for Cross-Couplings and Related Reactions in the 21st Century: A Critical Review. *Chem. Rev.* **2018**, *118*, 2249–2295.
- (15) Balanta, A.; Godard, C.; Claver, C. Pd nanoparticles for C-C coupling reactions. *Chem. Soc. Rev.* **2011**, *40*, 4973–4985.
- (16) Cano, R.; Schmidt, A. F.; McGlacken, G. P. Direct arylation and heterogeneous catalysis; ever the twain shall meet. *Chem. Sci.* **2015**, *6*, 5338–5346.
- (17) Hong, K.; Sajjadi, M.; Suh, J. M.; Zhang, K.; Nasrollahzadeh, M.; Jang, H. W.; Varma, R. S.; Shokouhimehr, M. Palladium Nanoparticles on Assorted Nanostructured Supports: Applications for Suzuki, Heck, and Sonogashira Cross-Coupling Reactions. *ACS Appl. Nano Mater.* **2020**, *3*, 2070–2103.
- (18) Bao, Y. S.; Zhaorigetu, B.; Agula, B.; Baiyin, M.; Jia, M. Aminolysis of aryl ester using tertiary amine as amino donor via C-O and C-N bond activations. *J. Org. Chem.* **2014**, *79*, 803–808.
- (19) Bao, Y.-S.; Wang, L.; Jia, M.; Xu, A.; Agula, B.; Baiyin, M.; Zhaorigetu, B. Heterogeneous recyclable nano-palladium catalyzed amidation of esters using formamides as amine sources. *Green Chem.* **2016**, *18*, 3808–3814.
- (20) Georgakilas, V.; Perman, J. A.; Tucek, J.; Zboril, R. Broad family of carbon nanoallotropes: classification, chemistry, and applications of fullerenes, carbon dots, nanotubes, graphene, nano-diamonds, and combined superstructures. *Chem. Rev.* **2015**, *115*, 4744–4822.
- (21) Gholinejad, M.; Naghshbandi, Z.; Nájera, C. Carbon-Derived Supports for Palladium Nanoparticles as Catalysts for Carbon-Carbon Bonds Formation. *ChemCatChem.* **2019**, *11*, 1792–1823.

- (22) Navalon, S.; Dhakshinamoorthy, A.; Alvaro, M.; Garcia, H. Metal nanoparticles supported on two-dimensional graphenes as heterogeneous catalysts. *Coord. Chem. Rev.* **2016**, *312*, 99–148.
- (23) Hargreaves, J. S. J. Heterogeneous catalysis with metal nitrides. *Coord. Chem. Rev.* **2013**, *257*, 2015–2031.
- (24) Ma, T. Y.; Liu, L.; Yuan, Z. Y. Direct synthesis of ordered mesoporous carbons. *Chem. Soc. Rev.* **2013**, *42*, 3977–4003.
- (25) Titirici, M. M.; Antonietti, M. Chemistry and materials options of sustainable carbon materials made by hydrothermal carbonization. *Chem. Soc. Rev.* **2010**, *39*, 103–116.
- (26) Zhao, Z.; Sun, Y.; Dong, F. Graphitic carbon nitride based nanocomposites: a review. *Nanoscale* **2015**, *7*, 15–37.
- (27) Li, M.; Li, Y.; Jia, L.; Wang, Y. Tuning the selectivity of phenol hydrogenation on Pd/C with acid and basic media. *Catal. Commun.* **2018**, *103*, 88–91.
- (28) Su, D. S.; Perathoner, S.; Centi, G. Nanocarbons for the development of advanced catalysts. *Chem. Rev.* **2013**, *113*, 5782–5816.
- (29) Felpin, F.-X.; Ayad, T.; Mitra, S. Pd/C: An Old Catalyst for New Applications - Its Use for the Suzuki-Miyaura Reaction. *Eur. J. Org. Chem.* **2006**, *2006*, 2679–2690.
- (30) Cao, Y.; Mao, S.; Li, M.; Chen, Y.; Wang, Y. Metal/Porous Carbon Composites for Heterogeneous Catalysis: Old Catalysts with Improved Performance Promoted by N-Doping. *ACS Catal.* **2017**, *7*, 8090–8112.
- (31) Bernsmeier, D.; Chuenchom, L.; Paul, B.; Rümmler, S.; Smarsly, B.; Kraehnert, R. Highly Active Binder-Free Catalytic Coatings for Heterogeneous Catalysis and Electrocatalysis: Pd on Mesoporous Carbon and Its Application in Butadiene Hydrogenation and Hydrogen Evolution. *ACS Catal.* **2016**, *6*, 8255–8263.
- (32) Wang, G. H.; Cao, Z.; Gu, D.; Pfander, N.; Swertz, A. C.; Spliethoff, B.; Bongard, H. J.; Weidenthaler, C.; Schmidt, W.; Rinaldi, R.; Schuth, F. Nitrogen-Doped Ordered Mesoporous Carbon Supported Bimetallic PtCo Nanoparticles for Upgrading of Biophenolics. *Angew. Chem. Ed. Int.* **2016**, *55*, 8850–8855.
- (33) Pérez-Rodríguez, S.; Pastor, E.; Lázaro, M. J. Ordered Mesoporous Carbon as a Support of Pd Catalysts for CO₂ Electrochemical Reduction. *Catalysts* **2020**, *10*, 912.
- (34) Wang, W.; Villa, A.; Kübel, C.; Hahn, H.; Wang, D. Tailoring the 3D Structure of Pd Nanocatalysts Supported on Mesoporous Carbon for Furfural Hydrogenation. *ChemNanoMat* **2018**, *4*, 1125–1132.
- (35) Zhong, L.; Chokkalingam, A.; Cha, W. S.; Lakhi, K. S.; Su, X.; Lawrence, G.; Vinu, A. Pd nanoparticles embedded in mesoporous carbon: A highly efficient catalyst for Suzuki-Miyaura reaction. *Catal. Today* **2015**, *243*, 195–198.
- (36) Pillo, Th.; Zimmermann, R.; Steiner, P.; Hüfner, S. The electronic structure of PdO found by photoemission (UPS and XPS) and inverse photoemission (BIS). *J. Phys.: Condens. Matter* **1997**, *9*, 3987–3999.
- (37) Bao, Y. S.; Baiyin, M.; Agula, B.; Jia, M.; Zhaorigetu, B. Energy-efficient green catalysis: supported gold nanoparticle-catalyzed aminolysis of esters with inert tertiary amines by C-O and C-N bond activations. *J. Org. Chem.* **2014**, *79*, 6715–6719.
- (38) Bao, Y. S.; Chen, C. Y.; Huang, Z. Z. Transesterification for synthesis of carboxylates using aldehydes as acyl donors via C-H and C-O bond activations. *J. Org. Chem.* **2012**, *77*, 8344–8349.
- (39) Li, J.; Shi, C.; Bao, A.; Jia, J. Development of Boron-Doped Mesoporous Carbon Materials for Use in CO₂ Capture and Electrochemical Generation of H₂O₂. *ACS omega* **2021**, *6*, 8438–8446.
- (40) Zhang, W.; Bao, Y.; Bao, A. Preparation of nitrogen-doped hierarchical porous carbon materials by a template-free method and application to CO₂ capture. *J. Environ. Chem. Eng.* **2020**, *8*, 103732.